

# RSC Advances



This is an *Accepted Manuscript*, which has been through the Royal Society of Chemistry peer review process and has been accepted for publication.

*Accepted Manuscripts* are published online shortly after acceptance, before technical editing, formatting and proof reading. Using this free service, authors can make their results available to the community, in citable form, before we publish the edited article. This *Accepted Manuscript* will be replaced by the edited, formatted and paginated article as soon as this is available.

You can find more information about *Accepted Manuscripts* in the [Information for Authors](#).

Please note that technical editing may introduce minor changes to the text and/or graphics, which may alter content. The journal's standard [Terms & Conditions](#) and the [Ethical guidelines](#) still apply. In no event shall the Royal Society of Chemistry be held responsible for any errors or omissions in this *Accepted Manuscript* or any consequences arising from the use of any information it contains.

## ARTICLE

## Recalcitrance of Cyanuric acid to Oxidative Degradation by OH Radical: Theoretical Investigation

Guangyan Liu

*Binzhou Polytechnic, Shandong 256603, China,  
gyliu2@yahoo.com*

### Abstract

Cyanuric acid (CA) is among the several organic compounds that are resistant to the oxidative degradation in advanced oxidation processes (AOPs). In the present study, the reaction between CA and  $\cdot\text{OH}$  radical (the primary reactive oxygen species in AOPs) were investigated by density functional theory and compared with that between 1,3,5-benzenetriol (BT) and  $\cdot\text{OH}$  radical. The results indicate that, comparing with BT, the two tautomers (enolic form and keto form) of CA are difficult thermodynamically and kinetically to react with  $\cdot\text{OH}$  radical via both the addition to triazine ring and electron abstraction. Although the reaction for the enolic form of CA was found to be much more favorable than its keto form, the less population of the enolic CA, due to its thermodynamic instability, makes it less competitive. The reason for the recalcitrance of CA to OH radical is attributed to the electron deficiency of triazine ring because of the higher electro negativity of N atom than that of C atom.

### 1. Introduction

Advanced oxidation processes (AOPs), such as semiconductor photocatalysis and (photo)-Fenton process, are considered as a kind of promising technologies for the treatment of wastewater, because nearly all kinds of organic compounds can be degraded, even mineralized by these processes. However, some organic compounds are exceptionally resistant to the oxidative degradation in AOP treatments. Among them, cyanuric acid (CA) is the most famous one, although it was reported to be degraded under some harsh conditions.<sup>1-3</sup> The recalcitrance of CA to  $\text{TiO}_2$  photocatalytic oxidation and Fenton process has been confirmed by comprehensive experimental facts.<sup>4-6</sup> Moreover, although s-triazine and other triazine-based herbicides and dyes undergo rapid degradation under AOP conditions, the degradation always stops at CA as the final product.<sup>7-9</sup>

Hydroxyl radical ( $\cdot\text{OH}$ ) is believed to be the primary reactive oxygen species in AOPs. The reactions between  $\cdot\text{OH}$  and organic compounds have been extensively studied by experimental and theoretical methods, and three possible pathways have been proposed: (1) addition to the aromatic ring, (2) electron transfer, and (3) H-atom abstraction.<sup>10</sup> Generally,  $\cdot\text{OH}$  reacts with aromatic substrates via pathways 1 and 2, while the last pathway is dominant for aliphatics. Therefore, when explaining the oxidative resistance of CA to  $\cdot\text{OH}$ , only the first two pathways were considered, and the proposed hypotheses include:<sup>11</sup> (1) the reaction between  $\cdot\text{OH}$  and CA is too slow to

compete with other processes, such as the recombination of photogenerated carriers and the coupling of  $\cdot\text{OH}$ ; (2)  $\cdot\text{OH}$  reacts with CA via electron transfer followed by  $\text{H}^+$  loss, but the formed radical is stable enough to avoid further oxidation before it re-couples with another electron or hydrogen atom; (3) the addition of  $\cdot\text{OH}$  to the CA ring does occur, but the adduct rapidly loses  $\cdot\text{OH}$  in a reversible way. Jenks, et al.<sup>11</sup> reported that no oxygen exchange between CA and  $\text{H}_2\text{O}$  was observed under photocatalytic condition (using  $^{18}\text{O}$ -enriched CA as the substrate), which excludes the third hypothesis. However, the question why CA is resistant to  $\cdot\text{OH}$  is still unclear and difficult to be answered by experimental methods. Alternatively, theoretical calculation is able to offer a complementary approach to gain deep insight into the mechanism behind the recalcitrance of CA. Although there are several theoretical studies on the reaction between  $\cdot\text{OH}$  and susceptible aromatic compounds, such as quinoline,<sup>12</sup> phenols,<sup>13</sup> benzene,<sup>14</sup> xylenes,<sup>15</sup> to the best of our knowledge, the reluctant reaction of CA has not been calculated yet.

In this work, in an attempt to elucidate the mechanism behind the recalcitrance of CA to AOPs, the  $\cdot\text{OH}$  addition and electron transfer pathways were examined by density functional theory. For comparison, the corresponding reactions of 1,3,5-benzenetriol (BT), which is iso-electronic and iso-symmetric with CA, was parallelly examined at the same theory level. Our results reveal that the reaction of CA with  $\cdot\text{OH}$  radical is difficult thermodynamically and kinetically for both the addition to triazine ring and electron abstraction, which provides a deeper insight into the resistance of CA to the oxidative degradation in AOPs.

## 2. Computational Methods

All geometry optimizations, harmonic vibrational frequencies, and zero-point energy (ZPE) calculations were performed by the density functional theory<sup>16, 17</sup> (DFT, with the B3LYP functional<sup>18-20</sup> and the 6-311++G(d,p) basis set). The minimum or transition state (TS) nature of stationary points was verified by frequency analysis. The effect of solvation was investigated with the most recent version of the polarizable continuum model, that is, integral equation formalism PCM (IEF-PCM)<sup>21</sup> to calculate the solvation free energies (geometry optimizations and frequency calculations were recalculated in water, the radii scale factor is 1.2<sup>22, 23</sup>). All the stationary point energies reported here have undergone a ZPE correction (unscaled), and all the energies are plotted relative to the total energy of initial reactants ( $\cdot\text{OH}$  and CA or BT). No symmetry was included in all the calculations.

To obtain the transition state, a search on potential surface was usually carried out by scanning the bond length of the forming C...OH or N...OH bond in the range of 1.3-2.4 Å, before the optimization of TS. Then, geometry optimizations were performed at the peak positions from this rough energy diagram, to obtain the exact structures and energies of transition states. Such strategy was always successful for the addition of  $\cdot\text{OH}$  to 1,3,5-benzenetriol and to the C position of CA. But For the  $\cdot\text{OH}$  addition to the N position of cyanuric acid, the length scan of the forming N-O bond showed that the energy increases monotonically with the shortening of N...OH distance, and no peak could be obtained.

The rate constants for the addition of  $\cdot\text{OH}$  to the aromatic ring were calculated by the classical

transition state theory according to the following equation:

$$k(\text{M}^{-1} \text{s}^{-1}) = \frac{k_b T}{h} \frac{Q_{\text{TS}}}{Q_{\text{R}} Q_{\cdot\text{OH}}} \exp\left(-\frac{E_0}{RT}\right),$$

where  $k_b$  is the Boltzmann constant,  $h$  is the Planck's constant,  $T$  is the temperature (298K),  $E_0$  is the reaction activation energy ( $E_{\text{TS}} - E_{\text{R}} - E_{\cdot\text{OH}}$ , including ZPE corrections),  $Q_{\text{TS}}$ ,  $Q_{\text{R}}$  and  $Q_{\cdot\text{OH}}$  are the total partition functions for TS, substrate (CA or BT) and  $\cdot\text{OH}$ , respectively. The Gaussian 03 package<sup>24</sup> was used for all calculations.

### 3. Results and discussion

#### 3.1. Substrate structure

CA is a weak acid in aqueous media ( $\text{pK}_{\text{a}1} = 7.0$ ,  $\text{pK}_{\text{a}2} = 11.3$ , and  $\text{pK}_{\text{a}3} = 14.5$ ). In aqueous solution, it exists as a mixture of tautomers, namely the enolic form (cyanuric acid, CAe) and keto form (isocyanuric acid, CAk). In alkaline condition, the enolic form is dominant, whereas in acidic media ( $\text{pH} < 6$ ), the keto form is more stable.<sup>1</sup> Accordingly, both the enolic form and keto form were examined in the present study. The optimized structures of CAk and CAe, as well as BT in both gas phase and water solution with selected bond lengths are shown in Fig. 1. It is found that the length for C–O bond in CAe and CAk are 1.332 (1.327) and 1.206 (1.217) Å (gas phase (water solution)), respectively, whereas the C–N bonds are 1.332 (1.334) and 1.391 (1.382) Å, respectively. It suggests that the C–O single bond in CAe transforms partly to the C=O double bond in CAk, and the aromaticity of C–N bonds in CA becomes lower, as the proton shifts from O atom to N atom. The C–O bond of CAe (1.332 (1.334) Å) is remarkably shorter than that of BT (1.367 (1.366)

Å), which means that the O atom of CAe participates in the conjugation system of aromatic ring to a larger extent than that of BT. The larger extend of O atom conjugation has an excess stabilization effect on the CAe molecule relative to BT. For these three molecules, the optimized structures in the gas phase and water solution are very close, indicating that the change of geometry caused by the solvation effect is not significant. The free energy comparison shows that, in both gas phase and water solution, CAk is more stable than CAe (by 30.1 and 29.3 kcal/mol, respectively), indicating CA exists mainly in the keto form at room temperature. This result is in consistent with earlier reports.<sup>1</sup> To give a more comprehensive understanding of the reaction of CA, both the reactions starting from CAk and CAe were studied in this work.

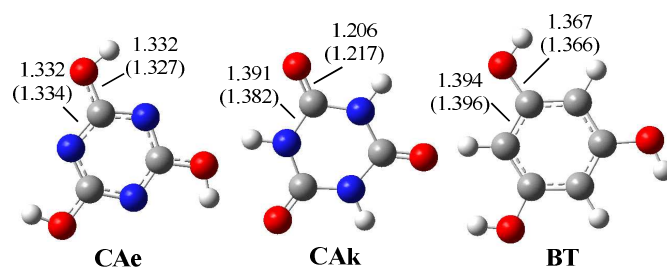


**Fig. 1** Optimized structures for CAe, CAk and BT in the gas phase and water solution (in parentheses) obtained at the B3LYP/6-311++G(d,p) level of theory. Atom representation: blue for N, gray for C, red for O, and white for H.

#### 3.2. $\cdot\text{OH}$ addition

Since  $\cdot\text{OH}$  reacts with aromatic substrates commonly via addition to the ring, we first examined the energy change accompanied with the formation of OH-adduct radical. CAe, CAk and BT all have two types of positions on the ring for

the attack of  $\cdot\text{OH}$  (C and N positions for CAe and CAk, ipso-C and ortho-C positions relative to hydroxyl for BT). Table 1 summarizes the thermodynamic function changes ( $\Delta H$ ,  $\Delta S$  and  $\Delta G$ ) and estimated equilibrium constants and the activation energy of the formation of OH-adduct radicals with different structures. For CAe and CAk, only the structures of C-OH adduct radicals could be optimized to a stationary point. The comparison of the energy of the formed HO-adduct radical with the sum of the energy of  $\cdot\text{OH}$  and substrate shows that the C-OH addition is endothermic with the enthalpy increase of 0.41 (3.83) and 6.27 (9.54) kcal/mol for CAe and CAk. The addition reactions have negative values of entropy change ( $\Delta S$ ), because the formed C-O/N-O bonds restrict the relative motion of  $\cdot\text{OH}$  and the substrate, and accordingly decrease the degree of freedom of system. Accordingly, the Gibbs energy changes ( $\Delta G$ s) of the calculated  $\cdot\text{OH}$  addition processes generally larger than that of the enthalpy changes ( $\Delta H$ s). The corresponding equilibrium constants are  $5.58 \times 10^{-8}$  ( $1.83 \times 10^{-10}$ ) and  $2.91 \times 10^{-13}$  ( $1.91 \times 10^{-15}$ ), respectively. The remarkable Gibbs free energy increase and the small equilibrium constants for the C-OH adducts indicate that this process is thermodynamically unfavorable and equilibrates near dissociative substrate and  $\cdot\text{OH}$ , especially for CAk, the dominant species under room temperature. For the  $\cdot\text{OH}$  addition to the N position, the energy increases with the shortening of N-O distance monotonically in the range of 1.3–2.4 Å, but no minima could be obtained (Fig. S1, ESI<sup>†</sup>). The energies in Table 1 for the N position addition were obtained with the fixation of the N–O bond at typical length (1.43 Å)<sup>25</sup> and indicate that this process is highly endothermic. The formidable of N position addition could be explained by the fact that the standard bond energy of N–O (55

kcal/mol) is much lower than that of C–O (85.5 kcal/mol),<sup>26</sup> and also by the high electronegativity of N atom. In contrast, the addition of  $\cdot\text{OH}$  to BT at both ipso-C and ortho-C positions are quite exothermic. The enthalpy changes ( $\Delta H$ ) for these two additions are -13.92 (-11.20) and -16.83 (-12.92) kcal/mol, respectively, which makes these processes proceed completely (with equilibrium constants of  $1.81 \times 10^3$  (16.3) and  $1.27 \times 10^5$  ( $2.81 \times 10^2$ )).

**Table 1** The thermodynamic function change ( $\Delta H$ ,  $\Delta S$  and  $\Delta G$ ), equilibrium constants, the activation energy and estimated rate constants for the  $\cdot\text{OH}$  addition.

Reactant	Product	g/s	$\Delta H^a$	$\Delta S^c$	$\Delta G^d$	$K$	$\Delta G^{2b}$	$K^e$
 CAe		g	0.41	-31.8	9.89	$5.58 \times 10^{-8}$	11.9	$2.15 \times 10^{-3}$
		s	3.83	-31.7	13.27	$1.83 \times 10^{-10}$	15.4	$6.40 \times 10^{-6}$
		g <sup>d</sup>	28.22	-35.1	38.69	$4.07 \times 10^{-29}$	-	---
		s <sup>d</sup>	36.54	-31.3	45.86	$2.26 \times 10^{-34}$	-	---
 CAk		g	6.27	-36.3	17.09	$2.91 \times 10^{-13}$	13.2	$1.99 \times 10^{-4}$
		s	9.54	-35.3	20.06	$1.91 \times 10^{-15}$	16.8	$5.20 \times 10^{-7}$
		g <sup>d</sup>	55.06	-33.7	65.12	$1.64 \times 10^{-48}$	-	---
		s <sup>d</sup>	63.38	-29.9	72.29	$9.08 \times 10^{-54}$	-	---
 BT		g	-13.92	-31.8	-4.44	$1.81 \times 10^3$	0.1	$2.31 \times 10^6$
		s	-11.20	-32.0	-1.65	16.3	1.9	$1.26 \times 10^5$
		g	-16.83	-33.1	-6.95	$1.27 \times 10^5$	-6.7	$1.65 \times 10^{11}$
		s	-12.92	-32.1	-3.34	$2.81 \times 10^2$	-4.8	$1.29 \times 10^{10}$

<sup>a</sup> The structure optimization and thermodynamic calculation were carried out with the length of the formed N–O bond fixed to 1.43 Å. <sup>b</sup> unit: kcal/mol; <sup>c</sup> unit: cal/mol/K, <sup>d</sup> unit:  $\text{M}^{-1} \text{s}^{-1}$

It should be noted that, in the C-OH adducts of CAe and CAk, the formed C–O bonds are 1.40 (1.40) and 1.39 (1.38) Å, respectively, shorter than those of  $\cdot\text{OH}$ -addition of BT (1.45 (1.45) Å for ipso-C and 1.46 (1.47) Å for ortho-C), which means that the thermodynamic difference shown in Table 1 cannot be attributed to the bond energy of the formed C–O bond. To explain the thermodynamic

difference in the  $\cdot\text{OH}$ -addition among CAe, CAk and BT, an examination on the electrostatic potential of these substrates were carried out (Fig. 2). The triazine ring in CA, especially for CAk, the more stable form, is more positive than the aromatic ring of BT. Quantitatively, the electron deficiency of the ring can be expressed with sum of the Mulliken charges of the atoms on the ring (six C atoms for BT, three C and three N atoms for CAe and CAk). The charge sums of the aromatic rings of BT, CAe and CAk are -0.617 (-0.819), -0.343 (-0.341) and -0.172 (-0.052), respectively, which shows that the triazine ring is much less negative than the benzene ring. Due to the electrophilic nature of  $\cdot\text{OH}$ , these results indicate that  $\cdot\text{OH}$  is more feasible to react with BT relative to the two forms of CA. Another line of explanation of the thermodynamic difference comes from the spin density analysis of the formed HO-adduct radicals (Fig. 3). For the C-OH adduct radical of CAe, ipso-C and ortho-C OH-adduct radicals of BT, the uncoupled electron distributes mainly around aromatic ring. In contrast, the uncoupled electron distributes primarily around the O atom bonded to the attacked C atom in the C-OH adduct radical of CAk, which may be caused by the single bond nature of C–N bond restricted the delocalization of the uncoupled electron around triazine ring. The localization of the uncouple electron could explain that the HO-addition to the C atom of CAk is the most energetically unfavorable one among these four tested processes.

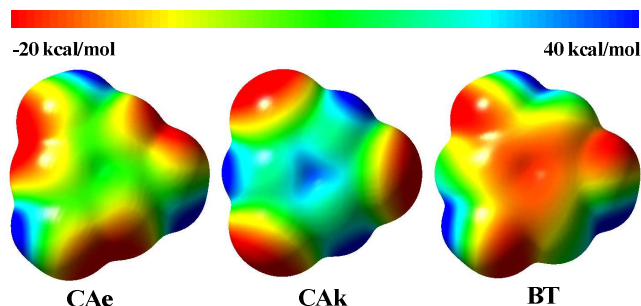


**Fig. 2** The electrostatic potential of CAe, CAk and BT, mapped on the surface of molecular electron density at isodensity of  $0.004 e\text{Bohr}^{-3}$ .

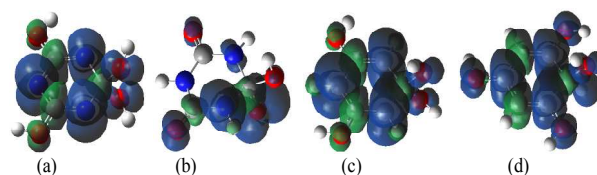


**Fig. 3** Spin density distribution of HO-adduct radicals. (a) C-OH adduct radical of CAe. (b) C-OH adduct radical of CAk. (c) ipso-C OH-adduct radical of BT. (d) ortho-C OH-adduct radical of BT.

Although a stable reactant complex is observed for the  $\cdot\text{OH}$  addition to the BT rings, no reactant complex for CA was obtained. This is evidently due to the electron deficiency of CA ring, which makes the stationary point for such complex on the potential surface disappears, because of the presence of other stronger interaction near the potential stationary point. In fact, all the effort to localize the reactant complexes between OH and CAe and CAk converged to H-bonding-based complex in which the OH radical interact with the proton of CA in the plane.

To investigate the kinetic characteristics of  $\cdot\text{OH}$  additions, the energy diagrams of these reactions were scanned. In both gas phase and water solution, typical reaction diagrams of reactant (R)—transition state (TS)—product (P) are shown for the  $\cdot\text{OH}$  additions to CAe and CAk (Figs. 4 and S2, ESI<sup>†</sup>). The TSs for the  $\cdot\text{OH}$  addition to CAe and CAk are located at 11.95 (15.39) and 13.17 (16.77) kcal/mol above the reactants (CA +  $\cdot\text{OH}$ ). The high energy barriers would make these  $\cdot\text{OH}$  addition processes kinetically reluctant. Estimated with TST, their rate constants are  $21.5 (1.99) \times 10^{-4}$  and  $64.0 (5.20) \times 10^{-7} \text{ M}^{-1} \text{ s}^{-1}$ , respectively, much lower than those of the reactions between  $\cdot\text{OH}$  and other

organics (normally  $10^7$ – $10^{10}$   $\text{M}^{-1} \text{s}^{-1}$ ).<sup>27</sup> The  $\cdot\text{OH}$  formed in the oxidation system would be primarily consumed by other coexist substrates or coupling with  $\text{H}_2\text{O}_2$  rather than induce the degradation of CA. In contrast, in the reaction between  $\cdot\text{OH}$  and BT, besides a shared reactant complex (RC), two low-lying TSs are located corresponding respectively to the ipso- and ortho-additions. The TS energy of the ipso-addition is slightly higher than that of the reactant (by 0.08 (1.94) kcal/mol), and the ortho-addition even gives a negative activation energy (-6.75 (-4.78) kcal/mol), which makes these two processes quite kinetically feasible with the estimated rate constants of  $23.1 (1.26) \times 10^5$  and  $16.5 (1.29) \times 10^{10}$   $\text{M}^{-1} \text{s}^{-1}$ , respectively. The rate constant of ortho-addition is much larger than that of the ipso-addition, showing that the  $\cdot\text{OH}$  addition would primarily take place at the ortho-site. This priority for the ortho-addition is in accordance with reported results,<sup>28, 29</sup> and may be explained with the ortho-para directing ability of the original hydroxyl groups and the electrophilic nature of  $\cdot\text{OH}$ .

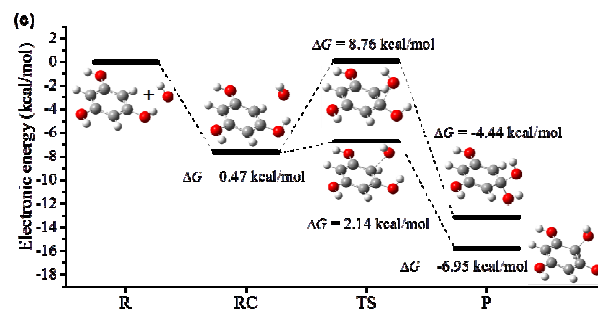
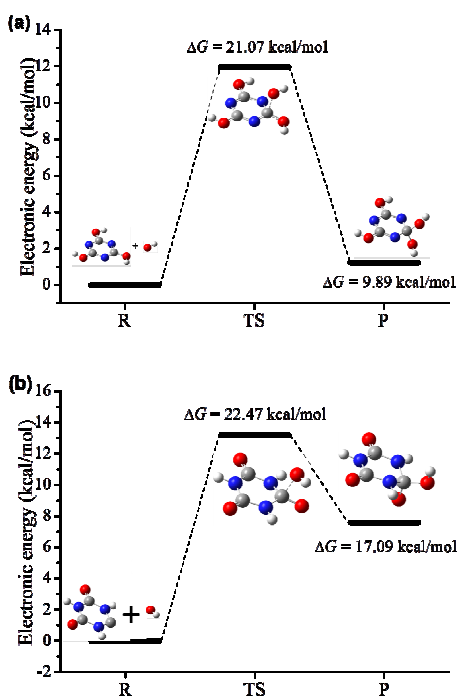


**Fig. 4** Energy diagram of  $\cdot\text{OH}$  addition to (a) CAe, (b) CAk, and (c) BT in gas phase.

A comparison of the structures of reactants, TSs and products clearly reveals the intermediate features of these TSs. For example, besides the forming of C–O bonds, the addition of  $\cdot\text{OH}$  to CAe mainly leads to a elongation of the two C–N bonds adjacent to the site of addition, which is a reflection of the electron transfer from the aromatic  $\pi$  orbitals to the newly formed C–O bonds. These C–N bonds are lengthened by 0.044 (0.044) Å from original CAe to TS, and by 0.067 (0.066) Å from the TS to HO-adduct radical ( $\Delta r_{\text{C-N}}^{\text{R} \rightarrow \text{TS}} / \Delta r_{\text{C-N}}^{\text{TS} \rightarrow \text{P}} = 0.66 (0.67)$ ). The  $\cdot\text{OH}$  addition to CAk causes the elongation of the C–O bond at the addition site. This bond is lengthened by 0.074 (0.065) Å from reactant to TS, and by 0.067 (0.075) Å from TS to the product ( $\Delta r_{\text{C-O}}^{\text{R} \rightarrow \text{TS}} / \Delta r_{\text{C-O}}^{\text{TS} \rightarrow \text{P}} = 1.10 (0.87)$ ). By contrast, the TSs for the  $\cdot\text{OH}$  addition to BT is more reactant-like, and the closeness for the ortho addition is more serious than the ipso one. For example, the C–C bonds adjacent to the added site (corresponding to the above-mentioned C–N bonds in the case of CAe) is lengthened by 0.026 (0.028) Å from original BT to TS and the lengthening is 0.072 (0.071) Å from the TS to the product in the ortho-attacking process ( $\Delta r_{\text{C-C}}^{\text{R} \rightarrow \text{TS}} / \Delta r_{\text{C-C}}^{\text{TS} \rightarrow \text{P}} = 0.36 (0.39)$ ). For the ipso-addition, the lengthening of adjacent C–C bonds is

0.037 (0.036) Å from original BT to TS and 0.067 (0.067) Å from the TS to the products ( $\Delta r_{C-C}^{R \rightarrow TS} / \Delta r_{C-C}^{TS \rightarrow P} = 0.55$  (0.54)). It is obvious that the ·OH addition to BT proceed via “early” TSs. These results are in accordance with Hammond’s postulate and the thermodynamic results that the ·OH addition to BT is more exothermic than the additions to CAe and CAk.

### 3.3. Electron Transfer

The possibility of the direct one-electron oxidation of CA (or BT) by ·OH is judged by the comparison of the ionization potentials (IPs) of CA (or BT) and the electron affinity of ·OH (Table 2). It is observed that the calculated EA of ·OH was 1.8 and 5.2 eV in the gas phase and water solution, respectively, which is comparable to the experimental values (1.9 and 6.3, respectively)<sup>30</sup> For all the three substrates (CAe, CAk and BT), the structures of their cationic radicals (Fig. S3, ESI†) were found to be very close to their neutral molecules, indicative of the low reorganization energy for the electron transfer. As shown in Fig. 2, the triazine rings of CAe and CAk are more positive than the benzene ring of BT, which suggests that CAs are more resistant to oxidation than BT. The calculation about the IPs of CAs and BT confirmed this assumption. In both gas phase and aqueous solution, the two forms of CA have similar IPs (10.0 (7.5) eV for CAe and 10.3 (7.8) eV for CAk), which are much higher than that of BT (8.1 (5.8) eV). The IPs of CAe, CAk and BT in the aqueous solution are about 2.3–2.5 eV lower than those in the gas phase, which is caused by the more remarkable stabilization effect of solvent on the cation than on neutral molecule and falls well in the range of 2–4 eV estimated by Pearson.<sup>31</sup> In both gas phase and aqueous solution, the EA of

·OH is much lower than the IPs of CAe and CAk, which means that the direct oxidation of the two forms of CA by ·OH is thermodynamically unfavorable. The EA of ·OH is still lower than the IP of BT but the difference is quite small particularly in the solution phase (5.2 vs 5.8 eV),, which is consistent with the estimation proposed by Tripathi:<sup>32</sup> whether electron transfer or addition is the first step in the reaction is determined by the IP of aromatic substrate, as most of the aromatic substrates (IP > 5.4 eV), BT reacts with ·OH through the addition of ·OH, rather than direct electron transfer.

**Table 2** The calculated IPs of CAe, CAk and BT and EA of ·OH

substrate	IP (eV)
CAe <sup>a</sup>	10.0 (7.5)
CAk <sup>a</sup>	10.3 (7.8)
BT <sup>a</sup>	8.1 (5.8)
OH <sup>b</sup>	1.8(5.2)

<sup>a</sup> ionization potentials; <sup>b</sup> electron affinity.

### 4. Conclusion

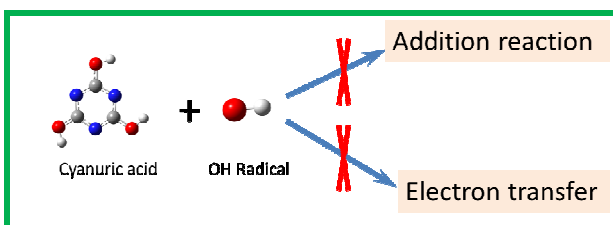
The theoretical calculations indicate that both the addition and electron transfer reaction between ·OH and CA is energetically unfavorable, which is attributed to the electron deficiency of triazine ring endowed by the high electronegativity of N atom. In agreement with the previous experimental observations, our results exclude the assumption that the addition of ·OH to the CA ring does occur, but the formed adduct rapidly loses ·OH in a reversible way. Moreover, other earlier mechanistic proposals for the resistance of CA to ·OH attack, such as the slow reaction rate and the stability of the CA radical formed through direct

oxidation followed by deprotonation, are also ruled out by the calculation.

## References

- E. Garcia-Lopez, G. Marci, N. Serpone and H. Hidaka, *J. Phys. Chem. C*, 2007, 111, 18025-18032.
- R. Varghese, U. K. Aravind and C. T. Aravindakumar, *J. Hazard. Mater.*, 2007, 142, 555-558.
- S. Horikoshi, Y. Wada, N. Watanabe, H. Hidaka and N. Serpone, *New J. Chem.*, 2003, 27, 1216 - 1223.
- A. Jańczyk, E. Krakowska, G. Stochel and W. Macyk, *J. Am. Chem. Soc.*, 2006, 128, 15574-15575.
- T. A. Tetzlaff and W. S. Jenks, *Org. Lett.*, 1999, 1, 463-466.
- N. Watanabe, S. Horikoshi, H. Hidaka and N. Serpone, *J. Photochem. Photobiol. A: Chem.*, 2005, 174, 229-238.
- C. L. Bianchi, C. Pirola, V. Ragaini and E. Selli, *Appl. Catal. B: Environ.*, 2006, 64, 131-138.
- E. Pelizzetti, V. Maurino, C. Minero, V. Carlin, M. L. Tosato, E. Pramauro and O. Zerbinati, *Environ. Sci. Technol.*, 1990, 24, 1559-1565.
- C. Hu, J. C. Yu, Z. Hao and P. K. Wong, *Appl. Catal. B: Environ.*, 2003, 42, 47-55.
- G. N. R. Tripathi, *J. Am. Chem. Soc.*, 1998, 120, 4161-4166.
- T. A. Tetzlaff and W. S. Jenks, *Org. Lett.*, 1999, 1, 463-466.
- A. R. Nicolaescu, O. Wiest and P. V. Kamat, *J. Phys. Chem. A*, 2005, 109, 2829-2835.
- M. Altarawneh, B. Z. Dlugogorski, E. M. Kennedy and J. C. Mackie, *J. Phys. Chem. A*, 2008, 112, 3680-3692.
- M. P. DeMatteo, J. S. Poole, X. Shi, R. Sachdeva, P. G. Hatcher, C. M. Hadad and M. S. Platz, *J. Am. Chem. Soc.*, 2005, 127, 7094-7109.
- J. Fan and R. Zhang, *J. Phys. Chem. A*, 2008, 112, 4314-4323.
- J. W. Labanowski and J. Andzelm, *Density Functional Methods in Chemistry*, Springer, New York, 1991.
- R. G. Parr and W. Yang, *Density Functional Theory in Atom and Molecules*, Oxford University Press, New York, 1989.
- A. D. Becke, *J. Chem. Phys.*, 1993, 98, 5648.
- A. D. McLean and G. S. Chandler, *J. Chem. Phys.*, 1980, 72, 5639.
- R. Krishnan, J. S. Binkley, R. Seeger and J. A. Pople, *J. Chem. Phys.*, 1980, 72, 650.
- M. Cossi, G. Scalmani, N. Rega and V. Barone, *J. Chem. Phys.*, 2002, 117, 43-54.
- V. Barone, M. Cossi and J. Tomasi, *J. Chem. Phys.*, 1997, 107, 3210-3221.
- R. Cammi, B. Mennucci and J. Tomasi, *J. Phys. Chem. A*, 2000, 104, 4690-4698.
- M. J. Frisch, G. W. Trucks, H. B. Schlegel, G. E. Scuseria, M. A. Robb, J. R. Cheeseman, J. J. A. Montgomery, T. Vreven, K. N. Kudin, J. C. Burant, J. M. Millam, S. S. Iyengar, J. Tomasi, V. Barone, B. Mennucci, M. Cossi, G. Scalmani, N. Rega, G. A. Petersson, H. Nakatsuji, M. Hada, M. Ehara, K. Toyota, R. Fukuda, J. Hasegawa, M. Ishida, T. Nakajima, Y. Honda, O. Kitao, H. Nakai, M. Klene, X. Li, J. E. Knox, H. P. Hratchian, J. B. Cross, V. Bakken, C. Adamo, J. Jaramillo, R. Gomperts, R. E. Stratmann, O. Yazyev, A. J. Austin, R. Cammi, C. Pomelli, J. W. Ochterski, P. Y. Ayala, K. Morokuma, G. A. Voth, P. Salvador, J. J. Dannenberg, V. G. Zakrzewski, S. Dapprich, A. D. Daniels, M. C. Strain, O. Farkas, D. K. Malick, A. D. Rabuck, K. Raghavachari, J. B. Foresman, J. V. Ortiz, Q. Cui, A. G. Baboul, S. Clifford, J. Cioslowski, B. B. Stefanov, G. Liu, A. Liashenko, P. Piskorz, I. Komaromi, R. L. Martin, D. J. Fox, T. Keith, M. A. Al-Laham, C. Y. Peng, A. Nanayakkara, M. Challacombe, P. M. W. Gill, B. Johnson, W. Chen, M. W. Wong, C. Gonzalez and J. A. Pople, Gaussian, Inc., Wallingford CT, 2004.
- W. J. Orville-Thomas, *Chem. Rev.*, 1957, 57, 1179-1211.
- R. T. Sanderson, *Chemical bonds and bond energy [by] R. T. Sanderson*, Academic Press, New York, 1971.
- G. V. Buxton, C. L. Greenstock, W. P. Helman and A. B. Ross, *J. Phys. Chem. Ref. Data*, 1988, 17, 513-886.
- C. Xu and L. Wang, *J. Phys. Chem. A*, 2013, 117, 2358-2364.
- G. Albarran and R. H. Schuler, *J. Phys. Chem. A*, 2007, 111, 2507-2510.
- P. Wardman, *J. Phys. Chem. Ref. Data*, 1989, 18, 1637-1755.
- R. G. Pearson, *J. Am. Chem. Soc.*, 1986, 108, 6109-6114.
- G. N. R. Tripathi, *J. Am. Chem. Soc.*, 1998, 120, 4161-4166.

## Table of Contents



Electron deficiency of triazine ring makes the reactions between cyanuric acid and OH radical energetically unfavorable.